Novel Sparse Model and Reconstruction for Dynamic Contrast-Enhanced MRI

Qiu Wang[1], Boris Mailhe[1], Robert Grimm[2], Marcel Dominik Nickel[2], Kai Tobias Block[3], Hersh Chandarana[3], and Mariappan S. Nadar[1]

[1]*Imaging and Computer Vision, Siemens Corporate Technology, Princeton, NJ, United States,* [2]*MR Application & Workflow Development, Siemens Healthcare, Erlangen, Germany,* [3]*Department of Radiology, New York University School of Medicine, New York, NY, United States*

Introduction: Dynamic contrast-enhanced (DCE) magnetic resonance imaging (MRI) is widely used in clinical practice, due to its ability to reveal clinically significant pathology which cannot be seen with conventional MRI [1]. Faster acquisition is critical since the acquisition has to be completed within a short time after contrast injection [2-4]. Sparse-model based reconstruction is one of the techniques to recover high quality image for accelerated acquisitions [5-6]. Sparse constraints correlated with the temporal dimension allow high spatio-temporal resolution [7]. This work proposes a new sparse model designed for DCE MRI reconstruction that leads to superior image quality and accurate time curves.

Figure 1

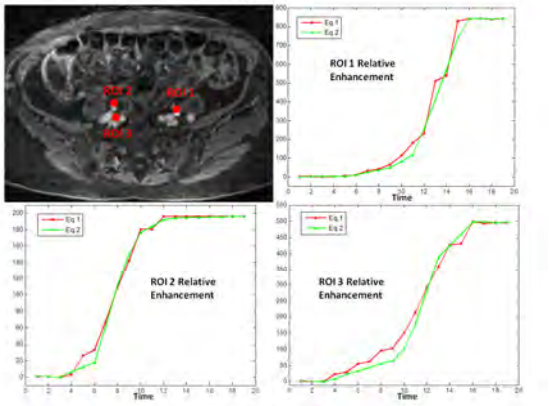

Methods: Reconstruction Model A fundamental sparse model for dynamic imaging is to impose sparsity along the spatial and temporal dimensions in a specific transform domain [8]. An example of reconstruction of such model is formulated as: $\min_x \frac{1}{2}\|F_{u,c}(x)-y\|_2^2+\lambda\|Wx\|_1$ (1), where x represents the images to be reconstructed, $F_{u,c}$ is the undersampled Fourier transform operator with coil profiles, y is the raw data, W represents a wavelet transform and λ is the regularization weight. This model enforces piece-wise constant intensities along the spatial and temporal directions. It is an efficient model for non-contrast-enhanced dynamic data. In the case of DCE MRI, the rapid variation of the intensity of the contrast agent leads to additional dynamics among phases. Following the previous model may fail to preserve the original dynamics in the contrast uptake, which are critical for clinical evaluation. To avoid this, one may consider adding a second regularization term that imposes piece-wise linearity instead of constant along time dimension. The new reconstruction is formulated as: $\min_x \frac{1}{2}\|F_{u,c}(x)-y\|_2^2+\lambda_1\|Wx\|_1+\lambda_2\|Tx\|_1$ (2), where λ_2 is the regularization weight and T is a second-order total variation [9] along the time dimension. This new model preserves the dynamics of the contrast uptake while efficiently suppresses fluctuations caused by noise.

Figure 2

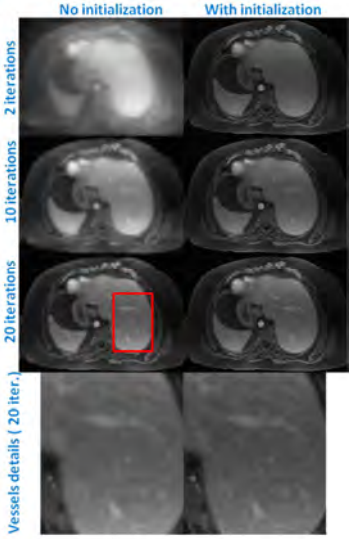

Initialization Algorithm Computational speedup is essential for a potential clinical application. The reconstruction speedup is achieved by computing an initial estimate of the images with lower computational cost in four steps. 1) Normalize the *k*-space samples to balance the contribution of darker pre-uptake and brighter post-uptake phases. 2) Group the normalized *k*-space samples from multiple temporal phases into a densely sampled *k*-space. 3) Do a single backward projection to solve for a single phase image x_0. 4) Scale x_0 by α_t for each temporal phase t to match the amplitude of its original measurement y_t (before normalization in step 1) by solving a closed-form least-squares problem: $\min_{\alpha_t \in R}\|y_t - F_{u,c}(\alpha_t x_0)\|_2^2$ (3).

Data & Experiments The proposed sparse model is demonstrated on a series of DCE data acquired with a non-product sequence using a stack-of-stars *k*-space trajectory [3,4], on a clinical 1.5 T (MAGNETOM Avanto) and a 3T (MAGNETOM Trio) scanner (Siemens Healthcare, Erlangen, Germany). Reconstruction is performed by solving Equation (1) and (2) using a prototype written in Matlab (The MathWorks, Natick, MA, USA). Time curve is derived by averaging tissue intensities within an ROI and plotted over time, and are normalized for the relative enhancement.

Figure 3

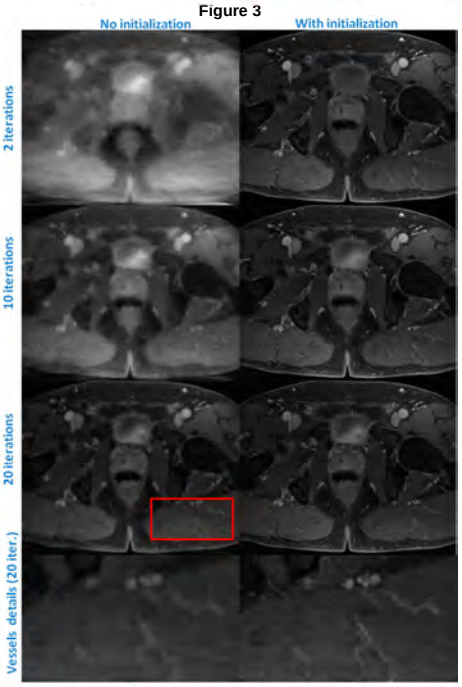

Results: Fig. 1 compares the time curves from reconstruction using Eq. 1 and Eq. 2 at three different ROIs (marked in red circles) from a pediatric liver data. The time curve from Eq. 1 reconstruction reveals stair-casing artifacts due to the promotion of piece-wise constant in the sparse model, while the time curve from Eq. 2 reconstruction records the continuous increase of the contrast uptake. Fig. 2a~2c shows image reconstruction through the model of Eq.2 with and without the initialization step on a different liver volunteer data at iterations 2, 10 and 20 of the iterative reconstruction. Image contrast and streaking artifacts are significantly reduced at different iterations when initialization is available. Fig. 2d shows the zoom-in of the liver region (marked in red in Fig. 2c) which compares the vessel details at 20 iterations. Fig. 3 is similar to Fig. 2 and demonstrates the image quality comparison from a prostate data.

Discussion and Conclusion: This work proposes a novel sparse model for DCE MRI reconstruction. Experimental results practically demonstrate the effectiveness of the proposed method in terms of better image quality and time curves. The proposed initialization method is novel with its special consideration for DCE data by computing separate temporal phases based on the raw data signal through a closed-form solution. In order to compensate for any possible early enhancement concerned with the initialization step, a pre-conditioning method [10] is utilized. Although the method is experimented on DCE MRI data, the sparse model and the initialization algorithm can be easily generalized to other types of dynamic imaging, e.g. perfusion MRI [11] or contrast enhanced imaging for other modalities.

References: [1] AR. Padhani, J Magn Reson Imaging 2002;16: 407–422. [2] B. Xu et al., Magn Reson Med 2013;69:370–381. [3] L. Feng et al., Magn Reson Med. 2014 Sep;72(3):707-17. [4] H. Chandarana, et al., Investigative Radiology, 2013. Jan;48(1):10-6. [5] M. Lustig et al., Magnetic Resonance in Medicine, 2007. [6] Q. Wang et al., Proc Intl Soc Mag Reson Med, #1549, 2014. [7] S. G. Lingala, et. al, Phys Med Biol 2013; 58:7309-7327. [8] J. Liu et al., Proc Intl Soc Mag Reson Med, #4249, 2012. [9] K. Bredies, et al., SIAM J. Imaging Sciences, 3(3):492–526, 2010. [10] B. Mailhe et al., Proc Intl Soc Mag Reson Med, 2015, submitted. [11] G. Adluru, et al., JMRM 2009 Jan;29(2):466-473.